Volume 34 June & December 2020 ISSN 0970-9169

GANITA SANDESH

गणित संदेश

A Half Yearly International Research Journal

of

Rajasthan Ganita Parishad

Registered Head Office

Department of Mathematics

SPC Government College, AJMER – 305001
(*INDIA*)

(NAAC Accredited "A" Grade College)

Website: www.rgp.co.in
E-mail: rgp@rgp.co.in

Issued December, 2023

E-mail: editor@rgp.co.in
E-mail: cmtr@rgp.co.in

GANITA SANDESH

गणित संदेश

Editorial Board

Editor: Dr. V. C. Jain

Associate Professor, Department of Mathematics, Engineering College Ajmer

E-mail: editor@rgp.co.in

Notes for contributors

1. The editors will be glad to receive contributions only from all parts of India / abroad in any area of Mathematics (Research / Teaching etc.).
2. Manuscripts for Publication should be sent through E-mail directly to the editor@rgp.co.in along with hard copy in Triplicate duly computerized with double spacing preferably with text in Times New Roman font 11pts. and Mathematical symbols(Math Type, Equation Editor or Corel equation).
3. Authors should provide abstract and identify 4 to 5 key words for subject classification.
4. Unduly long papers and papers with many diagrams / tables will not be normally accepted in general, length of the accepted paper should not exceed 10 printed pages.
4. The contributors are required to meet the partial cost of Publication at the rate of Rs. 200/- or equivalent US $ per printed page size A4 (even number pages) payable in advance.

Membership Fees / Subscription

	Period	**In India(Rs.)**	**Outside India(US $)**
Admission Fee / Enrolment Fee	First time only	100	100(or equivalent)
Life Membership		2000	2000(or equivalent)
Annual Membership fee for teachers(Colleges/Universities), T.R.F., Registered Research Scholars	Financial year	250	250(or equivalent)
Educational/ Research Institutions	Calendar year	500	500(or equivalent)

All payments must be made by Bank DD in favour of Rajasthan Ganita Parishad payable at AJMER or online State Bank of India Account No. 10200807636, IFSC Code: SBIN0000603 under intimation to the Treasurer, Rajasthan Ganita Parishad, Deptt. of Mathematics, SPC Govt. College, AJMER-305001(INDIA).

Ganita Sandesh Vol. 34 (June & December, 2020) pp. 1-12 ISSN : 0970-9169

DARK ENERGY STRING COSMOLOGICAL MODELS CONSIDERING BAROTROPIC FLUID DISTRIBUTION

Nikhil Jain

Department of Mathematics, Women Engineering College Ajmer

Email: jain10480@gmail.com

ABSTRACT

Bianchi type-VIII string cosmological model for barotropic fluid distribution with dark energy Λ are investigated.To get the deterministic model of the model, we assume that expansion θ is proportional to the shear (σ) and the dark energy (Λ) is assumed to be proportional to V^{-3} where V is scale factor. Various physical and geometrical properties of the model are also discussed.

Keywords: Bianchi VIII, string, barotropic fluid, dark energy, perfect fluid.

1. INTRODUCTION

It is believed that cosmic strings give rise to density perturbation which leads to the formation of galaxies (Zel'dovich [25]). The general relativistic treatment of strings was obtained by Letelier [9,10] and Stachel [21]. Bali et al. [1, 2, 3, 5] have obtained Bianchi type IX, type V & type I string cosmological models in general relativity. Exact solutions of string cosmology for Bianchi type II,VI_0, VIII and IX space-times have been obtained by Krori et al.[8]. Tyagi et al. [23] have studied Inhomogeneous Bianchi type-VI_0 string dust cosmological model of perfect fluid distribution in general relativity.Singh [20] also studied string cosmology with electromagnetic fields in Bianchi type-II, VIII & IX space times. Tyagi et al. [24] have studied Bianchi Type-IX String Cosmological Models for Perfect fluid Distribution in General Relativity.

A perfect fluid is an inviscid fluid with no heat conduction. It is analogous to an ideal gas in standard thermodynamics. The matter distribution is satisfactorily described by perfect fluids due to the large

scale distribution of galaxies in our universe. However, a realistic treatment of the problem requires the consideration of material distribution other than the perfect fluid.

The homogeneous and anisotropic Bianchi models play remarkable role in the present day universe. The advantages of the anisotropic models are that they have a significant role in the description of the evolution of the early phase of the universe and they help in finding more general cosmological models than the isotropic FRW models. Reddy et al. [16] studied Bianchi type II, VIII and IX models in scale covariant theory of gravitation. Chhajed et al. [6] have studied Bianchi type VIII cosmological model with Quadratic equation of state.Also Rao and Sanyasi Raju[15] and Sanyasi and Raju [19] have studied Bianchi type VIII & IX models in Zero mass scalar fields and in Self – Creation theory of Cosmology. Bali and Swati [4] have investigated Inflationary scenario in Bianchi type VIIIspace-time for a massless scalar field with flat potential. Rao et al. [12-14] have studied Bianchi type-II,VIII & IX string cosmological models , perfect fluid cosmological models in Saez Ballester scalar tensor theory of gravitation and string cosmological models in general relativity as well as self-creation theory of gravitation respectively.

We consider two cases (i)$\boldsymbol{\rho + \lambda = 0}$(Reddy string) (ii)$\boldsymbol{\rho - \lambda = 0}$ (Nambu string). To get the deterministic model of the universe, we assume that the shear (σ) is proportional to expansion (θ) as considered by Thorne [22] and Collins et al. [7]**.** The physical and geometrical properties of the models are discussed.

2. METRIC AND FIELD EQUATIONS

The line –element for Bianchi type-VIII space time is considered as

$$ds^2 = -dt^2 + A^2(t)[d\theta^2 + cosh^2\theta d\emptyset^2] + B^2(t)[d\Psi + sinh\theta d\emptyset]^2 (1)$$

in which *A(t), B(t)* are cosmic scale functions.

The energy momentum tensor T_i^j in the presence of perfect fluid is defined by

$$T_i^j = (\rho + p)v_i v^j + p g_i^j - \lambda x_i x^j \tag{2}$$

Where ρ is proper energy density, p is pressure and λ is string tension density. Also x^i, the unit space like vector specifying the direction of strings and v^i, the unit time like vector specifying the following conditions

$v_i v^i = -1 = -x_i x^i$ and $v^i x_i = 0$

The co-moving coordinate system is chosen as

$v^i = (0,0,0,1)$ and $x^i = \left(\frac{1}{B}, 0,0,0\right)$

The Einstein's field equation in the geometrized unit $(c = 8\pi G = 1)$ is given by

$$R_i^j - \frac{1}{2} R g_i^j + \Lambda g_i^j = -T_i^j \tag{3}$$

Where R_i^j is Ricci tensor, $R = g^{ij} R_{ij}$ is Ricci scalar.

The Einstein's field equations (3) for metric (1) leadto:

$$\frac{2A_{44}}{A} + \frac{{A_4}^2}{A^2} - \frac{1}{A^2} - \frac{3B^2}{4A^4} + \Lambda = -(p - \lambda) \tag{4}$$

$$\frac{A_4 B_4}{AB} + \frac{B^2}{4A^4} + \frac{B_{44}}{B} + \frac{A_{44}}{A} + \Lambda = -(p) \tag{5}$$

$$\frac{{A_4}^2}{A^2} + \frac{2A_4 B_4}{AB} - \frac{1}{A^2} - \frac{B^2}{4A^4} + \Lambda = \rho \tag{6}$$

The scalar expansion θ and shear σ are given by

$$\theta = 3\mathrm{H} \tag{7}$$

$$\sigma^2 = \frac{1}{2}\left[\sum_{i=1}^{3} H_i^2 - \frac{1}{3}\theta^2\right] \tag{8}$$

3. SOLUTION OF FIELD EQUATIONS

The field equations (4) to (6) represent a system of three independent equations in six unknowns *A*, *B*, λ, *p*, ρ and Λ .

In order to overcome the undeterminacy of six unknowns involved in three independent field equations, we consider the following two cases (i) $\rho + \lambda = 0$, i.e. the sum of the rest energy density and tension density for a cloud of strings vanishes (Reddy [17, 18] and Mohanty[11]) (ii) (Nambu) strings given by $\rho - \lambda = 0$.

Two additional constraints related to these parameters are required to obtain the explicit solution of the system.

Cosmic shear σ represents an effect of distortion of the image of distant galaxies due to deflection of light by matter, as predicted by general relativity.

Metric expansion θ is a key feature of Big-Bang cosmology and is modeled mathematically with the Friedmann- Lemaitre- Robertson-Walker (FLRW) metric. The metric expansion of space is the averaged increase of metric (i.e.) measured distance between distant objects in the universe with time.

We assume that shear σ is proportional to expansion θ

Thus we have

$$B = A^n \tag{9}$$

and Λ is proportional to

$$\Lambda = \frac{\alpha}{SA^2} \tag{10}$$

Where $\alpha$is a constant of proportionality.

We assume the above conditions under two cases

(i) Case I: $\boldsymbol{\rho + \lambda = 0}$

From (4) and (6)

$$\frac{2A_{44}}{A} + \frac{2A_4^2}{A^2} - \frac{2}{A^2} - \frac{B^2}{A^4} + \frac{2A_4B_4}{AB} + 2\wedge = -p \quad (11)$$

Using (5), we get

$$\frac{A_{44}}{A} + \frac{2A_4^2}{A^2} - \frac{2}{A^2} - \frac{5}{4A^{4-2n}} + \frac{A_4B_4}{AB} - \frac{B_{44}}{B} + \wedge = 0 \quad (12)$$

Using condition (9) and (10), we get

$$\frac{(1-n)A_{44}}{A} + \frac{(2+2n-n^2)A_4^2}{A^2} = \frac{2}{A^2} + \frac{5A^{2n-4}}{4} - \frac{\alpha}{A^{n+2}} \quad (13)$$

$$A_{44} + \frac{(n^2-2n-2)A_4^2}{(n-1)A} = \frac{2}{(1-n)A} + \frac{5A^{2n-3}}{4(1-n)} - \frac{\alpha}{(1-n)A^{n+1}} \quad (14)$$

Now let us consider $A_4 = f(R)$ and $A_{44} = ff'$ in equation (14) we get

$$ff' + \frac{(n^2-2n-2)f^2}{(n-1)R} = \frac{2}{(1-n)R} + \frac{5A^{2n-3}}{4(1-n)} - \frac{\alpha}{(1-n)A^{n+1}} \quad (15)$$

Equation (15) can be written in the form

$$\frac{df^2}{dA} + \frac{2(n^2-2n-2)f^2}{(n-1)A} = \frac{4}{(1-n)A} + \frac{5A^{2n-3}}{2(1-n)} - \frac{2\alpha}{(1-n)A^{n+1}} \quad (16).$$

After integration, Eq. (16) leads to

$$f^2 = \frac{M}{A^{\frac{2(n^2-2n-2)}{(n-1)}}} - \frac{2}{(n^2-2n-2)} - \frac{5A^{\frac{(2n^2-4n+2)}{(n-1)}}}{2(4n^2-8n-2)} + \frac{2\alpha}{(n^2-3n-4)A^n} \quad (17)$$

where *M* is the integrating constant.

from equation (17), we have

$$\int \frac{dR}{\sqrt{A^{\frac{M}{\frac{2(n^2-2n-2)}{(n-1)}}-\frac{2}{(n^2-2n-2)}-\frac{5A^{\frac{(2n^2-4n+2)}{(n-1)}}}{2(4n^2-8n-2)}+\frac{2\alpha}{(n^2-3n-4)A^n}}}} = \int dt + M' = t + M' \quad (18)$$

WhereM' is the integrating constant. Value of A can be obtained from equation (18). Hence by appropriate transformation of co-ordinates, the metric (1) leads to the form

$$ds^2 = -\frac{dT^2}{\left[T^{\frac{M}{\frac{2(n^2-2n-2)}{(n-1)}}-\frac{2}{(n^2-2n-2)}-\frac{5T^{\frac{(2n^2-4n+2)}{(n-1)}}}{2(4n^2-8n-2)}+\frac{2\alpha}{(n^2-3n-4)T^n}}\right]} + T^2[d\theta^2 + cosh^2\theta d\emptyset^2] \; +$$

$$T^{2n}[d\Psi + sinh\theta \mathrm{d}\emptyset]^2 \quad (19)$$

(ii) Case II: $\boldsymbol{\rho - \lambda = 0}$

From (4) and (6)

$$\frac{2A_4B_4}{AB} + \frac{B^2}{2A^4} - \frac{2A_{44}}{A} = p \quad (20)$$

Using (5), we get

$$\frac{2nA_4^2}{A^2} + \frac{3}{4A^{4-2n}} - \frac{A_{44}}{A} + \frac{A_4B_4}{AB} + \frac{B_{44}}{B} + \frac{\alpha}{A^{n+2}} = 0 \quad (21)$$

Using condition (9) and (10), we get

$$\frac{(n-1)A_{44}}{A} + \frac{(2n+n^2)A_4^2}{A^2} = -\frac{3A^{2n-4}}{4} - \frac{\alpha}{A^{n+2}} \quad (22)$$

$$A_{44} + \frac{(n^2+2n)A_4^2}{(n-1)A} = -\frac{3A^{2n-3}}{4(n-1)} - \frac{\alpha}{(n-1)A^{n+1}} \quad (23)$$

Now let us consider $A_4 = f(A)$ and $A_{44} = ff'$ in equation (23) we get

$$ff' + \frac{(n^2+2n)f^2}{(n-1)A} = -\frac{3A^{2n-3}}{4(n-1)} - \frac{\alpha}{(n-1)A^{n+1}} \quad (24)$$

Equation (24) can be written in the form

$$\frac{df^2}{dA}+\frac{2(n^2+2n)f^2}{(n-1)A}=-\frac{3A^{2n-3}}{2(n-1)}-\frac{2\alpha}{(n-1)A^{n+1}} \tag{25}$$

After integration, Eq. (25) leads to

$$f^2=\frac{N}{A^{\frac{2(n^2+2n)}{(n-1)}}}-\frac{2\alpha}{(n^2+5n)A^n}-\frac{3A^{\frac{(2n^2-4n+2)}{(n-1)}}}{2(4n^2+2)} \tag{26}$$

Where N is the integrating constant.

From equation (26), we have

$$\int \frac{dR}{\sqrt{\frac{N}{A^{\frac{2(n^2+2n)}{(n-1)}}}-\frac{2\alpha}{(n^2+5n)A^n}-\frac{3A^{\frac{(2n^2-4n+2)}{(n-1)}}}{2(4n^2+2)}}}=\int dt+N'=t+N' \tag{27}$$

Where N' is the integrating constant. Value of A can be obtained from equation (27). Hence by appropriate transformation of co-ordinates, the metric (1) leads to the form

$$ds^2=-\frac{dT^2}{\left[\frac{N}{T^{\frac{2(n^2+2n)}{(n-1)}}}-\frac{2\alpha}{(n^2+5n)T^n}-\frac{3T^{\frac{(2n^2-4n+2)}{(n-1)}}}{2(4n^2+2)}\right]}+T^2[d\theta^2+cosh^2\theta d\emptyset^2]\ +T^{2n}[d\Psi+$$

$$sinh\theta \mathrm{d}\emptyset]^2 \tag{28}$$

4. PHYSICAL AND GEOMETRICAL CHARACTERISTICS

For the model (19), energy density (ρ), pressure (p), expansion (θ), shear tensor (σ), string tension density (λ) are given by

$$\rho = \frac{M(2n+1)}{T^{\frac{(2n^2-2n-6)}{(n-1)}}} + \frac{\alpha(n+2)(n-1)}{(n-4)(n+1)T^{n+2}} - \frac{1}{4T^{4-2n}} - \frac{n(n+2)}{(n^2-2n-2)T^2} - \frac{5(2n+1)T^{\frac{(2n^2-6n+4)}{(n-1)}}}{4(2n^2-4n-1)} \quad (29)$$

$$\lambda = \frac{1}{4T^{4-2n}} - \frac{M(2n+1)}{T^{\frac{(2n^2-2n-6)}{(n-1)}}} - \frac{\alpha(n+2)(n-1)}{(n-4)(n+1)T^{n+2}} + \frac{n(n+2)}{(n^2-2n-2)T^2} + \frac{5(2n+1)T^{\frac{(2n^2-6n+4)}{(n-1)}}}{4(2n^2-4n-1)} \quad (30)$$

The directional Hubble parameters H_x, H_y, H_z are given by

$$H_x = H_y = \frac{\dot{A}}{A} \quad (31)$$

$$H_z = \frac{\dot{B}}{B} = \frac{n\dot{A}}{A} \quad (32)$$

The mean Hubble parameter (H) is given by

$$H = \frac{1}{3}\left(H_x + H_y + H_z\right) = \frac{(n+2)\dot{A}}{3A} \quad (33)$$

$$\theta = (n+2)\left[\frac{M}{T^{\frac{2(n^2-n-3)}{(n-1)}}} - \frac{2}{(n^2-2n-2)T^2} - \frac{5}{2(4n^2-8n-2)T^{4-2n}} + \frac{2\alpha}{(n^2-3n-4)T^{n+2}}\right]^{\frac{1}{2}} \quad (34)$$

$$\sigma^2 = \frac{(n-1)^2}{3}\left[\frac{M}{T^{\frac{2(n^2-n-3)}{(n-1)}}} - \frac{2}{(n^2-2n-2)T^2} - \frac{5}{2(4n^2-8n-2)T^{4-2n}} + \frac{2\alpha}{(n^2-3n-4)T^{n+2}}\right] \quad (35)$$

Isotropic pressure p is determined if fluid is known to obey an equation of state of the form

$p = \gamma\rho\,, where\ \ 0 \le \gamma \le 1$ (36)

Equation (36) lead to

$$p = \gamma\left(\frac{M(2n+1)}{T^{\frac{(2n^2-2n-6)}{(n-1)}}} + \frac{\alpha(n+2)(n-1)}{(n-4)(n+1)T^{n+2}} - \frac{1}{4T^{4-2n}} - \frac{n(n+2)}{(n^2-2n-2)T^2} - \frac{5(2n+1)T^{\frac{(2n^2-6n+4)}{(n-1)}}}{4(2n^2-4n-1)}\right)$$

(37)

For the model (28), energy density (ρ), pressure (p), expansion (θ), shear tensor (σ), string tension density (λ) are given by

$$\rho = \lambda = \frac{N(2n+1)}{T^{\frac{(2n^2+6n-2)}{(n-1)}}} - \frac{\alpha(n^2+n-2)}{(n^2+5n)T^{n+2}} - \frac{(n+2)(n+1)}{2(2n^2+1)T^{4-2n}} - \frac{1}{T^2} \quad (38)$$

$$p = \gamma\left(\frac{N(2n+1)}{T^{\frac{(2n^2+6n-2)}{(n-1)}}} - \frac{\alpha(n^2+n-2)}{(n^2+5n)T^{n+2}} - \frac{(n+2)(n+1)}{2(2n^2+1)T^{4-2n}} - \frac{1}{T^2}\right) \quad (39)$$

$$\boldsymbol{\theta = (n+2)\left[\frac{N}{T^{\frac{(2n^2+6n-2)}{(n-1)}}} - \frac{3}{2(4n^2+2)T^{4-2n}} - \frac{2\alpha}{(n^2+5n)T^{n+2}}\right]^{\frac{1}{2}}} \quad (40)$$

$$\sigma^2 = \frac{(n-1)^2}{3}\left[\frac{N}{T^{\frac{(2n^2+6n-2)}{(n-1)}}} - \frac{3}{2(4n^2+2)T^{4-2n}} - \frac{2\alpha}{(n^2+5n)T^{n+2}}\right] \quad (41)$$

$$\Lambda = \frac{\alpha}{T^{n+2}} \quad (42)$$

5. CONCLUSION

The models (19) and (28) start expanding with big-bang at *T=0.*The expansion θ decreases as time increases for $-2 < n < 2$. We also observe that it approaches to zero as $T \to \infty$ and stops when $n = -2$. Since $\to \infty, \frac{\sigma}{\theta} \neq 0$, therefore the model does not approach isotropy for large value of T, however the model is isotropize for $n = 1$.

The energy density(ρ), string tension density (λ) and pressure(p) for both models are found to be a decreasing function of time T for $-2 < n < 2$ and approaches to 0 as$T \to \infty$.

By equation (42) , we observe that the cosmological term ∧ for the model is also decreasing function of time T for $n > -2$ and approaches to zero at late time , which in agreement with present astronomical observations.

Hence, in general, the present model represents expanding, shearing and non-rotating, anisotropic universe.

REFERENCES

[1] Bali, R. and Anjali, Bianchi type-I magnetized string cosmological models with bulk viscous fluid in general relativity. Astrophysics Space Sci. 302, 201-206, 2006.

[2] Bali, R. and Dave, S., Bianchi type-IX string cosmological models with bulk viscous fluid in general relativity. Astrophysics Space Sci 288, 503-509, 2003.

[3] Bali, R. and Singh, D. K., Bianchi type-V bulk viscous fluid string dust cosmological model in general relativity. Astrophysics Space Sci. 300, 387-394, 2005.

[4] Bali, R. and Swati, Bianchi type VIII Inflationary Universe with Massless Scalar Field in General Relativity. Prespacetime Journal, vol. 6 (8), pp. 679-683, 2015.

[5] Bali, R. and Upadhyay, R.D., LRS Bianchi Type-I String Dust Magnetized Cosmological Model in General Relativity. Astrophysics. Space Sci. 283, 97-108, 2003.

[6] Chhajed, D., Sharma, A. & Chouhan, D.S., Bianchi type VIII cosmological model with Quadratic equation of state. Prespacetime journal USA, vol. 8, No.7, 2017.

[7] Collins, C.B., Glass, E.N. and Wilkinson, D.A., Exact Spatially Homogeneous Cosmologies. Gen. Relativ. Gravit, 12 805, 1980.

[8] Krori, K.D., Chaudhury, T., Mananta, C. R. and Mazumdar, A., Some exact solutions in string cosmology. Gen. Rel. Grav. 22, 123-130, 1990.

[9] Letelier, P.S., Clouds of strings in general relativity. Phys. Rev. D 20, 1249, 1979.

[10] Letelier, P.S., String Cosmologies. Phys. Rev. D 28, 2414, 1983.

[11] Mohanty, G., Sahoo, R.R. and Mahanta K.L., Five dimensional LRS Bianchi type I string cosmological model in Saez and Ballester theory, Astrophys. Space Sci. 312, 321-324, 2007.

[12] Rao, V.U.M., Santhi, M.V. and Vinutha, T., Exact Bianchi type-II, VIII & IX String cosmological models in Saez –Ballester theory of gravitation. Astrophysics and space science , vol. 314, No. 1-3, pp. 73-77,2008.

[13] Rao,V.U.M , Santhi,M.V. and Vinutha,T. , Exact Bianchi type- II,VIII & IX perfect fluid cosmological models in Saez Ballester theory of gravitation . Astrophysics and Space science, vol. 317, no. 1-2, pp. 27-30,2008.

[14] Rao, V.U. M. , Santhi, M.V. and Vinutha, T., Exact Bianchi type-II, VIII and IX string cosmological models in General Relativity and self-creation theory of gravitation. Astrophysics and space science, vol. 317, N0. 1-2, pp. 83-88, 2008.

[15] Rao, V.U.M. and Sanyasi Raju, Y.V. S. S. Exact Bianchi type VIII and IX models in the presence of zero –mass scalar field's .Astrophysics and space Science, vol. 187, no.1, pp. 113-117, 1992.

[16] Reddy, D.R.K., Patrudu, B.M., and Venkateswarlu, R., Exact Bianchi type II, VIII & IX cosmological model in scalar- covariant theory of gravitation. Astrophysics and Space Science, vol.204, no.1, pp.155-160, 1993.

[17] Reddy D R K., A String Cosmological model in Brans-Dicke theory of gravitation, Astrophysics Space Science, vol 286 , pp. 365-371, 2003.

[18] Reddy D R K., On Einstein-Rosen Cosmic String in a scalar tensor theory of gravitation. Astrophysics Space Science,vol 305, pp. 139-141, 2006.

[19]

[20] Sanyasi Raju, Y.V. S. S. and Rao, V. U. M., Exact Bianchi type VIII & IX models in the presence of the self-creation theory of cosmology. Astrophysics and Space Science, vol. 189, no.1, pp. 39-43, 1992.

[21] Singh, G.P., String cosmology with Electromagnetic fields in Bianchi type II, VIII, IX space times, Nuovo Cimento B110, 1463-1471, 1995.

[22] Stachel, J., Thickening the string. I. the string perfect dust. Phys. Rev. D 21, 2171, 1980.

[23] Thorne K.S., Primordial element formation, Primordial magnetic Fields, and the isotropy of the Universe.The Astrophysical Journal, vol. 148, pp. 51-68, 1967.

[24] Tyagi, A., Sharma, A. and Chhajed, D., Inhomogeneous Bianchi Type-VI_0 String Dust Cosmological Model of Perfect Fluid Distribution in General Relativity. Journal of Rajasthan Academy of Physical Sciences, vol. 14, pp. 15-23, 2015.

[25] Tyagi, A., Sharma, K. and Jain, P., Bianchi Type-IX String Cosmological Models for Perfect fluid Distribution in General Relativity. Chinese Physics Letter, 27, 079801, 2010.

[26] Zel'dovich, Ya. B., Cosmological fluctuations produced near a singularity .Monthly Notices of the Royal Astronomical Society, 192, 663-668, 1980.

Ganita Sandesh Vol. 34 (June & December, 2020) pp. 13-22 ISSN : 0970-9169

STANDARD AND NON-STANDARD VARIANCE SCHEME

RekhaRani[1],Dr.MahenderSingh Poonia[2]

[1]Research Scholar, Department of Mathematics, OM Sterling Global University, Hisar,Haryana,India

[2]Professor, Department of Mathematics, OM Sterling Global University, Hisar, Haryana,India

Email: [1]rekhaverma2591@gmail.com;[2]drmahender@osgu.ac.in

Abstract:In this research, our nonstandard finite variance scheme is developed to solve the nonlinear reaction-diffusion problem. The lemma for the discretization equation that is connected to the positivity and roundedness requirement will be presented in this section of the essay. Several branches of research and engineering need the use of reaction-diffusion equations. Their solutions frequently have a variety of physical characteristics. Three of these qualities are replicated by novel non-standard finite difference schemes that we create in a methodical manner. The first characteristic is the stability or instability of the relateduniverse independent equation's fixed points. There are presented numerical experiments.

Keywords:finite difference scheme, reaction-diffusion problem, two-stage

1. Introduction:

Several branches of research and engineering need the use of reaction-diffusion equations. Their solutions frequently have a variety of physical characteristics. Three of these qualities are replicated by novel non-standard finite difference schemes that we create in a methodical manner. The first characteristic is the stability or instability of the related space independent equation's fixed points. Non-standard single and two-stage theta approaches that are existing in the context of stiff or non-stiff differential equation organisations maintain this attribute. By using non-local estimate of nonlinear responses, schemes are created for the associated stationary equations that respect the principle of energy conservation (second property).Theta-methods in the period variable are combined with energy-preserving structures in the space mutable to produce non-standard structures that, when the step sizes

are properly related functionally, show the boundedness besides positivity of the solution. Also, an appropriate non-standard scheme in the periodcapricious is described along with a spectral technique in the intergalactic variable. There are presented numerical experiments.In order to solve the nonlinear reaction-diffusion equation, we create a nonstandard version of the finite difference structure.

In this section of the paper, we will state the lemma associated to the positivity too boundedness requirement for the discretization equation. For the purpose of determining whether or not the lemma is accurate, we simulate some numerical results. The nonlinear reaction-diffusion partial differential equation is what we focus on in this discussion. In order to design and investigate a solution to the problem at hand, a novel nonstandard finite difference technique is developed.

Evgeniya et al. (2021) conducted research on diffusion processes, which are significant in many fields, such as chemistry, astronomy, metallurgy, medication, and extra areas. This paper investigates and resolves the issue of charged particle dispersion in a semi-infinite thin tube under the influence of an electromagnetic field. In this chapter, Wang et al. (2020) examine many ODE models on behalf of the diffusion of revolution and epidemiological representations. They examine various ordinary differential equation models for the diffusion of inventions while reviewing the conventional notion of innovation diffusion with an emphasis on online social networks.

Khan and Aziz (2018) In this paper, a one-dimensional and two-dimensional hyperbolic partial technique for generating equations is examined, along with a HAAR wavelet-based collocation strategy for numerical solution of diffusion. The numerical consequences support the accuracy, effectiveness, and sturdiness of the suggested technique.

Gunvant (2016) aims to solve the first initial boundary value problem (IBVP) on behalf of the semi-linear variable order fractional diffusion equation numerically by a variety of finite difference methods. The Fourier method is used to examine the stability and convergence of this procedure. Finally, using MATLAB, the answer to a few numerical situations is investigated and visually shown.

According to D'Ambrosio and Paternoster (2014), the goal of this study is to solve partial differential equations that simulate the diffusion problem accurately and quickly using gradually improved numerical solutions. A numerical study demonstrates that using a general-purpose solution is substantially less efficient and accurate when used for both temporal and spatial problems. Tory and Bargie (2015) It is possible to rewrite the nonlinear diffusing equation in a way that leads directly to its stochastic equivalent. By replicating the

schedules of molecules, the stochastic slant helps us comprehend the physical developmentbetter. The parallel implementation of our approach is quite effective. The hemitrope analysis method (HAM) was utilised in this study by Fallahzadeh and Shakibi (2015) to determine the series solution of the linear Convection Diffusion (CD) equation.

The study by Gurarslan and Sari (2011) provided suitable solutions for both linear and nonlinear diffusion problems. In order to solve some equations, processes using various universal quadrature techniques in space and robust stability preservation Runge-Kutta techniques were applied. To produce prototypes that are far more realistic, this method may be used to various nonlinear ordinary differential equations.

According to Griffiths and Schiesser (2012), the one-dimensional (1D) diffusion equation is a straightforward parabolic PDE that allows for travelling wave solutions.

Nonlinear Reaction-Diffusion Partial Differential Equation

We construct the nonlinear reaction-diffusion calculation; a nonstandard determinate difference approach has been used. For the discretization equation, we have given the lemma relating the positivity and boundedness conditions. To ensure that the lemma is accurate, we simulate some numerical outcomes.

Nonstandard Finite Alteration Scheme on behalf of a Nonlinear PDE

We reflect the reaction-diffusion equation below, which includes a nonlinear cubic basis term:

$$u_t = u_{tt} - (u - a_1)(u - a_2)(u - a_3)$$

Employment of Standard Finite Variance Method on behalf of Reaction-Diffusion Equation

For equation, we give a typical finite variance approach. The first derivative of our discrete model have been created using a forward difference scheme, while the second derivative have been constructed using a central difference method.

$$\frac{u_m^{n+1} - u_m^n}{\Delta t} = \frac{u_{m+1}^n - 2u_m^n + u_{m-1}^n}{(\Delta x)^2} - (u_m^n)^3 + (u_m^n)$$

Employment of Nonstandard Finite VarianceProcess for Reaction-Diffusion Equation

The following discrete model for equation have been chosen based on past work on non-standard finite variancearrangements and the application of a positivity disorder.

$$\frac{u_m^{n+1} - u_m^n}{\Delta t} = \frac{u_{m+1}^n - 2u_m^n + u_{m-1}^n}{(\Delta x)^2} - \left(\frac{3u_m^{n+1} - u_{m-1}^n}{2}\right)(u_{m-1}^n)^2 + u_{m-1}^n$$

A comparison will be made between the partial differential equation under consideration and the standard finite-difference schemes. This comparison will focus on how the explanations

of the several nonstandard besides standard distinct models contrastafter one another.The first IBVPaimed at nonlinear time fractional diffusion equation (FDE) is studied numerically in this section. Consider the form of the nonlinear time FDE.

$D_t^a u(x,t) = \frac{\partial^2 u^m}{\partial x^2}, m \geq 2, x \in (a,b), 0 < t \leq T$ (1)

with initial condition$u(x,0) = g(x), x \in (a,b)$ (2)

boundary conditions$u(a,t) = u(b,t) = 0, t > 0$ (3)

The nonlinear periodFDE is known as the first IBVP. For m = 1, the above equation (3) is reduced to a linear time fractional diffusion equation, which is investigated numerically using the Neummann boundary condition. We now present a numerical method for simulating the nonlinear behaviour of the nonlinear first IBVP (3)-based nonlinear system (2). Let $x_i = ih(i = 0,1,\ldots,M) and t_k = k_T(k = 0,1,\ldots,N), where h = \frac{b-a}{M} and \tau = \frac{T}{N}$be the spatial and temporal approximation to$u(x_i,t_k)$The equation (4.25) is discretized as follows::

$$\frac{\partial^a u(x_i,t_{k+1})}{\partial t^a} = \frac{\theta\delta_x^2(u_{i,k+1}^m) + (1-\theta)\delta_x^2(u_{i,k}^m)}{h^2} \quad (4)$$

Where θ is weight factor$(0 \leq 1-\theta \leq 1)$which regulate the degree of implicitness For$\theta = 0, \frac{1}{2} and\ 1$ provides the obvious, and completelyimplied finite difference approaches, in that order. As a result, the weighted average finite difference method is a broader FDE. The subsequent scheme approximates the time FDE in equation (3): As a result, we can write it. as$u_{i,k} = u(x_i,t_k) weget$

$\frac{\partial^\alpha u}{\partial t^\alpha} = \frac{\tau^{-\alpha}}{\Gamma(2-\alpha)}\left[u_{i,k+1} - u_{i,k}\right] + \frac{\tau^{-\alpha}}{\Gamma(2-\alpha)}\sum_{i=1}^{k}\left[u_{i,k+1-j} - u_{i,k-j}\right]b_j$ (5)

Where $b_j = (j+1)^{1-a} - j^{1-a}, j = 0,1,2,\ldots,k$.We can solve equation (6) using the time fractional approximation.

$$\frac{\tau^{-\alpha}}{\Gamma(2-\alpha)}\left[u_{i,k+1} - u_{i,k}\right] + \frac{\tau^{-\alpha}}{\Gamma(2-\alpha)}\sum_{j=1}^{k} b_j \times \left[u_{i,k+1-j} - u_{i,k-j}\right] = \frac{\theta\delta_x^2(u_{i,k+1}^m) + (1-\theta)\delta_x^2(u_{i,k}^m)}{h^2}$$

Rearranging the above equation yields

$$u_{i,k+1} - u_{i,k} = r\theta\delta_x^2(u_{i,k+1}^m) + r(1-\theta)\delta_x^2(u_{i,k}^m) - \sum_{j=1}^{k}\left[u_{i,k+1-j} - u_{i,k-j}\right]b_j$$

Where $r = \frac{T^a\Gamma(2-a)}{h^2}$The nonlinear term in the preceding equation is$(\delta_x^2(u_{i,k+1}^m))$ make it difficult to find the solution to an equation (6). To avoid this problem, the nonlinear term is

used. $(\delta_x^2(u_{i,k+1}^m))$ is linearized using the procedure described previously for integer order nonlinear partial differential equations. The nonlinear term is linearized $\delta_x^2(u_{i,k+1}^m)$by extending Taylor's series about the point (i, k), we have

$$u_{i,k+1}^m = u_{i,k}^m + k\frac{\partial u_{i,k}^m}{\partial t} + \frac{k^2}{2!}\frac{\partial^2 u_{i,k}^m}{\partial t^2} + \cdots$$
$$= u_{i,k}^m + k\frac{\partial u_{i,k}^m}{\partial u_{i,k}}\frac{\partial u_{i,k}}{\partial t} + \cdots$$

Which, when truncated up to order k, gives us

$$u_{i,k+1}^m + u_{i,k}^m + mu_{i,k}^{m-1}(u_{i,k+1} - u_{i,k}) \qquad (7)$$

Equation (7) in equation (6) yields

$$u_{i,k+1} - u_{i,k} = r\theta\delta_x^2\left(u_{i,k}^m + mu_{i,k}^{m-1}(u_{i,k+1} - u_{i,k})\right) + r(1-\theta)\delta_x^2(u_{i,k}^m) - \sum_{j=1}^{k}[u_{i,k+1} - u_{i,k-j}]\,b_j \qquad (8)$$

Putting $w_i = u_{i,k+1} - u_{i,k}$ in equation (8), we obtain

$$w_i = r\theta\delta_x^2(mu_{i,k}^{m-1}w_i) + r\delta_x^2(u_{i,k}^m) - \sum_{j=1}^{k}[u_{i,k+1} - u_{i,k-j}]\,b_j \qquad (9)$$

We have used central difference to create

$$-mr\theta w_{i-1}u_{i-1,k}^{m-1} + (1 + 2mr\theta u_{i,k}^{m-1})w_i - mr\theta w_{i+1}u_{i+1,k}^{m-1} = ru_{i-1,k}^m - 2ru_{i,k}^m + ru_{i+1,k}^m - \sum_{j=1}^{k}[u_{i,k+1-j} - u_{i,k-j}]b_j \qquad (10)$$

When we substitute m = 2 in equation (10), we get

$$-2r\theta w_{i-1}u_{i-1,k} + (1 + 4r\theta u_{i,k})w_i - 2r\theta w_{i+1}u_{i+1,k} = ru_{i-1,k}^2 - 2ru_{i,k}^2 + ru_{i+1,k}^2 - \sum_{j=1}^{k}[u_{i,k+1-j} - u_{i,k-j}]b_j \qquad (11)$$

For $k = 0, i = 1, 2, \ldots, M-1$ The equation (11) can be written in the (M-1) equation system. The system's matrix equation is as follows.

$$AW = BU_0 + b \qquad (12)$$

Where $A = \begin{pmatrix} 1 + 4r\theta u_{1,0} & 2r\theta u_{2,0} & & \\ -2r\theta u_{1,0} & 1 + 4r\theta u_{2,0} & 2r\theta u_{3,0} & \\ & -2r\theta u_{M-3,0} & 1 + 4r\theta u_{M-2,0} & 2r\theta u_{M-1,0} \\ & & -2r\theta u_{M-2,0} & 1 + 4r\theta u_{M-1,0} \end{pmatrix}$

$$B = \begin{pmatrix} -2ru_{1,0} & ru_{2,0} & & & \\ ru_{1,0} & -2ru_{2,0} & ru_{3,0} & & \\ & \cdot & \cdot & \cdot & \\ & & ru_{M-3,0} & -2ru_{M-2,0} & ru_{M-1,0} \\ & & & ru_{M-2,0} & -2ru_{M-1,0} \end{pmatrix}$$

$$W = [w_1, w_1, \dots., w_{M-1}]^T, U_0 = [u_{1,0}, u_{2,0}, \dots., u_{M-1,0}]^T$$

$$b = [ru_{0,0}^2 + 2r\theta u_{0,0}(u_{0,1} - u_{0,0}), 0, \dots 0, ru_{M,0}^2 + 2r\theta u_{M,0}(u_{M,1} - u_{M,0})]^T$$

Before writing the system of (M − 1) equations for k ≥ 1, The last term of the equation (12) is rearranged as follows.

$$\sum_{j=1}^{k} [u_{i,k+1-j} - u_{i,k-j}]b_j = b_1 u_{i,k} + \sum_{j=1}^{k-1} (b_{j+1} - b_j)u_{i,k-j} - b_k u_{i,0} \quad (13)$$

Equation substitution (13) We obtain in equation (11),

$$-2r\theta w_{i-1}u_{i-1,k} + (1 + 4r\theta)w_i u_{i,k} - 2r\theta w_{i+1}u_{i+1,k} = ru_{i-1,k}^2 - 2ru_{i,k}^2 + ru_{i+1,k}^2 - b_1 u_{i,k} - \sum_{j=1}^{k-1} (b_{j+1} - b_j)u_{i,k-j} + b_k u_{i,0} \quad (14)$$

Putting $k = 1, i = 1, 2, \dots, M - 1$ in equation (14), we obtain

$$-2r\theta w_0 u_{0,1} + (1 + 4r\theta u_{1,1})w_1 - 2r\theta w_2 u_{2,1} = ru_{0,1}^2 - 2ru_{1,1}^2 + ru_{2,1}^2 - b_1 u_{1,1} + b_1 u_{1,0}$$

$$-2r\theta w_1 u_{1,1} + (1 + 4r\theta u_{2,1})w_1 - 2r\theta w_3 u_{3,1} = ru_{1,1}^2 - 2ru_{2,1}^2 + ru_{3,1}^2 - b_1 u_{2,1} + b_1 u_{2,0}$$

$$-2r\theta w_{M-2}u_{M-2,1} + (1 + 4r\theta u_{M-1,1})w_{M-1} - 2r\theta w_M u_{M,1} = ru_{M-2,1}^2 - 2ru_{M-1,1}^2 + ru_{M,1}^2 - b_1 u_{M-1,1} + b_1 u_{M-1,0}$$

Matrix equations can be used to represent the system of (M −1) equations

$$AW = CU_1 + b_1 U_0$$

Similarly, for $k = 2$, the matrices equation

$$AW = CU_2 + c_1 U_1 + d_2 U_0$$

In general, for each $k \geq 1, (k = 1, 2, \dots, N)$ The matrix equation can be expressed as follows:

$$AW = CU_k + c_1 U_{k-1} + c_2 U_{k-2} + c_3 U_{k-3} + \cdots + c_k U_1 + b_k U_0 \quad (15)$$

Where

$$C = \begin{pmatrix} -2ru_{1,1} - b_1 & ru_{2,1} & & & \\ ru_{1,1} & -2ru_{2,1} - b_1 & ru_{3,1} & & \\ & \cdot & \cdot & & \\ & & ru_{M-3,1} & -2ru_{M-2,1} - b_1 & ru_{M-1,1} \\ & & & ru_{M-2,1} & -2ru_{M-1,1} - b_1 \end{pmatrix}$$

$W = [w_1, w_1, \dots., w_{M-1}]^T, c_k = b_k - b_{k+1}$

$U_k = [u_{1,k}, u_{2,k}, \dots, u_{M-1,k}]^T$

Theorem: Conditionally stable is the weighted average finite difference scheme (13).

Proof. The following two examples demonstrate the stability of the model.

Case-I For$k = 0$, the equation of a matrix (13) is

$$AW = BU_0 + b$$

B is a column matrix, and A and B are tridiagonals. It can be written as

$$(I - 2rc\theta T_{M-1})(u_{k+1} - u_k) = rcu_k T_{M-1}$$

Where

$$T_{M-1} = \begin{pmatrix} -2 & 1 & & & \\ 1 & -2 & 1 & & \\ & & \cdot & \cdot & \\ & & 1 & -2 & 1 \\ & & & 1 & -2 \end{pmatrix}$$

$c = \max_{i,k}\{u_{i,k}\}$ and I is identity matrix

$$(I - 2rc\theta T_{M-1})(u_{k+1} - u_k) = \left(rcT_{M-1} + (I - 2rc\theta T_{M-1})\right)u_k$$

$$u_{k+1} = \frac{I + (1-2\theta)rcT_{M-1}}{I - 2rc\theta T_{M-1}}u_k$$

The following are the matrices eigenvalues:

$$\lambda_s = \frac{1-4rc(1-2\theta)\sin^2\left(\frac{s\pi}{2M}\right)}{1+8rc\theta\sin^2\left(\frac{s\pi}{2M}\right)}, s = 1(1)(M-1) \qquad (16)$$

The eigenvalue for the stability condition is$-1 \leq \lambda \leq 1$. We only need to prove that one side of the inequality is trivial $-1 \leq \lambda$

We can deduce the following from equation (16).

$$-1 \leq \frac{1 - 4rc(1-2\theta)\sin^2\left(\frac{s\pi}{2M}\right)}{1 + 8rc\theta\sin^2\left(\frac{s\pi}{2M}\right)}$$

$$-1 - 8rc\theta\sin^2\left(\frac{S\pi}{2M}\right) \leq 1 - 4rc(1-2\theta)\sin^2\left(\frac{S\pi}{2M}\right)$$

$$-1 - 16rc\theta\sin^2\left(\frac{s\pi}{2M}\right) \leq 1 - 4rc\sin^2\left(\frac{s\pi}{2M}\right)$$

$$-1 - 4rc(4\theta - 1)\sin^2\left(\frac{s\pi}{2M}\right) \leq 1$$

$$4rc(1-4\theta)\sin^2\left(\frac{s\pi}{2M}\right) \leq 2$$

$$r \leq \frac{1}{2c(1-4\theta)\sin^2\left(\frac{s\pi}{2M}\right)}\left(0 \leq \theta < \frac{1}{4}\right)$$

Case-II For $k \geq 1$, (16) is a matrix equation.

$$AW = CU_k + c_1U_{k-1} + c_2U_{k-2} + c_3U_{k-3} + \cdots + c_kU_1 + b_kU_0, k \geq 1$$

$$C = \begin{pmatrix} -2ru_{1,1} - b_1 & ru_{2,1} & & & \\ ru_{1,1} & -2ru_{2,1} - b_1 & ru_{3,1} & & \\ & \cdot & \cdot & \cdot & \\ & & ru_{M-3,1} & -2ru_{M-2,1} - b_1 & ru_{M-1,1} \\ & & & ru_{M-2,1} & -2ru_{M-1,1} - b_1 \end{pmatrix}$$

It is possible to write it as

$$(I - 2rc\theta T_{M-1})(u_{k+1} - u_k) = (rcT_{M-1} + (I - 2rc\theta T_{M-1}) - b_1)u_k$$

$$u_{k+1} = \frac{(I - b_1) + (1 - 2\theta)rcT_{M-1}}{I - 2rc\theta T_{M-1}} u_k$$

The matrix C eigenvalues are

$$\lambda_s = \frac{(1-b_1) - 4rc(1-2\theta)\sin^2\left(\frac{s\pi}{2M}\right)}{1+8rc\theta\sin^2\left(\frac{s\pi}{2M}\right)}, s = 1(1)(M-1) \quad (17)$$

One aspect of inequality is insignificant. We only demonstrate $-1 \leq \lambda$. We can deduce from equation (17), that

$$-1 \leq \frac{(1 - b_1) - 4rc(1 - 2\theta)\sin^2\left(\frac{s\pi}{2M}\right)}{1 + 8rc\theta\sin^2\left(\frac{s\pi}{2M}\right)}$$

$$-1 - 8rc\theta\sin^2\left(\frac{s\pi}{2M}\right) \leq (1 - b_1) - 4rc(1 - 2\theta)\sin^2\left(\frac{s\pi}{2M}\right)$$

$$\cdot$$

$$-1 - 4rc(4\theta - 1)\sin^2\left(\frac{s\pi}{2M}\right) \leq (1 - b_1)$$

$$4rc(1 - 4\theta)\sin^2\left(\frac{s\pi}{2M}\right) \leq (2 - b_1)(1 - b_1)$$

$$r \leq \frac{s\pi}{4c(1 - 4\theta)\sin^2\left(\frac{s\pi}{2M}\right)}\left(0 \leq \frac{1}{4}\right)$$

As a consequence, we settle that the future weighted average finite difference scheme is only stable under certain conditions.

$$r \leq \frac{(1 - b_1)}{4c(1 - 4\theta)Sin^2\left(\frac{s\pi}{2M}\right)}, \left(0 \leq \theta < \frac{1}{4}\right) for\ 0 < a < 1$$

We further developed the nonstandard determinate difference approach for the nonlinear reaction-diffusion PDE. Because the new approach is basically explicit, it is straightforward to apply in order to obtain numerical solutions and it readily meets the positivity and boundedness constraints. This new scheme also includes the necessary fixed points. Numerous computer evaluations have shown that the resulting nonstandard scheme is more capable of approaching the precise solution than the traditional finite difference discretization of the issue.

2. Conclusion:

An unconventional finite difference technique on behalf of the Fisher equation serves as the inspiration for this paper. Below a specific functional relationship amid the period and space step sizes, the aforementioned arrangement is stable with regard to the boundedness besides positivity nose. We have suggested a methodical process for creating novel qualitatively stable systems for broad reaction-diffusion equations that incorporate subjectiveanswer terms consuming a considerablemeeker functional relative. In the process, we developed more universaluncomplicated stable non-standard structures of theta sort for stiff and non-stiff organisations of ODE, as well as energy-preserving outlineson behalf of a class of Hamiltonian arrangements.We have created a different approach for the general diffusion equation. The stiffness chin of the linearized arrangement of Fourier factors is precisely fused into both the spectral approach (in the interstellar variable) besides the non-standard FDE (in the period variable). Our future strategy consists of two parts. First, how does the analysis in this study apply to the creation of schemes that exhibit the roundedness and positive properties of solutions to the Burger equation and the convective equation that were both taken into consideration in. The notionalparts of the ethereal non-standard approach shown here will be discussed next.

3. References:

1) Bargieł, M., and Tory, E. M. (2015). Solution of linear and nonlinear diffusion problems via stochastic Differential Equations. Computer Science, 16(4), 1-15.
2) Birajdar, Gunvant. (2016). Finite Difference Schemes for Variable Order Time-Fractional First Initial Boundary Value Problems. Applications and Applied Mathematics: An International Journal, 12. 112-135.
3) Aziz, I., and Khan, I. (2018). Numerical Solution of Diffusion and Reaction–Diffusion Partial Integro-Differential Equations. International Journal of Computational Methods, 15(6), https://doi.org/10.1142/S0219876218500470.
4) Fallahzadeh, A., and Shakibi, K. (2015). A method to solve Convection-Diffusion equation based on homotope analysis method. Journal of Interpolation and Approximation in Scientific Computing, 1-8.
5) D'Ambrosio, R. and Beatrice, P. (2014). Numerical solution of a diffusion problem by exponentially fitted finite difference methods. Springer Plus. 3(425), 1-7.
6) Griffiths, G. and Schiesser, W. (2012). Linear Diffusion Equation. Traveling Wave Analysis of Partial Differential Equations, 47-55.

7) Taira, Kazuaki. (2021). Diffusion Processes and Partial Differential Equations by Kazuaki Taira (z-lib.org), 16-23.
8) Wang, H., Wang, F., and Xu, K. (2020). Ordinary Differential Equation Models on Social Networks. Springer International Publisher, 1-200.
9) Volodina, Evgeniya & Mikishanina, E. (2021). The diffusion problem. Journal of Physics: Conference Series. 1889. 022083. 10.1088/1742-6596/1889/2/022083.
10) Gurarslan, G. and Sari, M. (2011). Numerical solutions of linear and nonlinear diffusion equations by a differential quadrature method. International Journal for Numerical Methods in Biomedical Engineering. 27. 69 - 77.

Ganita Sandesh Vol. 34 (June & December, 2020) pp. 23-37 ISSN : 0970-9169

Analysis Complex Behavior of Some Discrete and Continuous Nonlinear Dynamical System

A.K. Chaudhary[1], Pankaj Narang[2], Saureesh Das[3] and M.K.Das[3]

[1] Department of Physics, Sri Venkateswara College

University of Delhi South Campus, New Delhi-110021.

[2] Department of Physics, ARSD College

University of Delhi South Campus, New Delhi-110021.

[3] Institute of Informatics & Communication

University of Delhi South Campus,

Benito-Juarey Road, New Delhi-110021

ABSTRACT

Complexity analysis of some discrete and continuous nonlinear dynamical systems have been numerically explored using methods such as Gottwald's 0-1 test and Shanon's entropy. For discrete nonlinear case, a Logistic map and a Henon'smap has been considered while for continuous nonlinear case a sinusoidally excited Duffing oscillator is chosen. Gotwald's 0-1 chaos test and Shanon's entropy have been extensively used to identify different domains of regular dynamics and chaotic states and their transitions as a result of varying the values of the control parameter(s) in both Logistic system, Henon 2D map and excited Duffing system. The methods used in the analysis are shown to work directly on the time-series and found to be very successful in rightly characterizing the dynamical complexities in these systems.

Key words: Discrete, continuous ,entropy, chaos, complexity, Nonlinear dynamics.

1. Introduction

A pre-requisite for development of a nonlinear model is its accurate characterization. In experiments exhibiting chaos, it is necessary to detect it in real-time observation of the system on varying the control parameter of the system. In the last two decades, chaos detection has been found to play an important role in understanding the complexities of dynamics observed in the several areas, eg. physics [1], chemistry [2], economics [3], biology[4] etc.Determining the Lyapunov characteristic exponent provides a most popular method for detection of chaos [5] but due to some limitations several other methods have also been suggested in the literature [6-7].Besides these methods, Gottwald [8-11] proposed a 0-1 chaos test (01CT, here after), which is simple and can be applied to any observed or simulated data from a dynamical system.

In this work, we describe the main features of the 01CT and apply it to both simulated data from known nonlinear discrete maps such as Logistic 1D-map, Henon's 2D-map and continuous system such as an excited Duffing system. Shanon's entropy has also been used to further supplement the 01CT method and use of these methods have been shown to be directly applicable to the time sequence of the foregoing systems and very effective in characterizing regular and chaotic dynamics.

Beside the foregoing preliminary description, this paper is organized as follows. In section 2, we briefly outline the $0-1$ chaos test (01CT) [8-11] and also the Shanon's entropy method (SE) [4] to identify regimes of regular, quasiperiodic and chaotic observed in discrete and continuous nonlinear dynamical system. In section 3,as a case study, we select the Logistic and Henon map as specific example of discrete nonlinearsystemand sinusoidally excited Duffing equation for continuous system and further describe results of applying 01CT and SE to the foregoing nonlinear systems. Section 4 summarizes the findings of various case studies describe in section 3.

2. Methods of Characterizing the Regular and Chaotic Dynamics

In this paper, we use the 01CT and SE to characterize the onset of regular and chaotic state in nonlinear dynamical system defined in terms of discrete maps and continuous evolving states.These test are briefly outlined in the following.

2a. Description of 0-1 chaos test

In this section, we provide the outlinesand some features of 0-1 chaos test recipe that characterizes or distinguishes the regular dynamics from chaotic behavior of deterministic system. The 0-1 chaos test [8-11] is in fact a binary test and is suitably designed for analysis of deterministic systems. Such a test in fact compliments discrete and continuous nonlinear dynamical system and may be of use in discussion regarding the solar system stability on one side to cardiac arrhythmias on the other [9]. One of the

importantfeaturesof the 01CT is its applicability to both discrete and continuous deterministic systemand further its implementation does not rest on the nature of the non-linear dynamical system [9].

(A) Computation of translational variables

For a given time sequence, $X(j), j = 1, \ldots, N$, following translational variables are defined,

$$p_c(n) = \sum_{j=1}^{n} X(j)\cos(jc)$$
$$q_c(n) = \sum_{j=1}^{n} X(j)\sin(jc) \quad (1)$$

where $c\,\epsilon(0, \pi)$ and $n = 1,2, \ldots, N$. For typical systems such as 1D Logistic map, as described in the following section, Fig.1 displays the plots of $p_c(n)$ and $q_c(n)$obtained in the foregoing system exhibiting regular and chaotic dynamics.

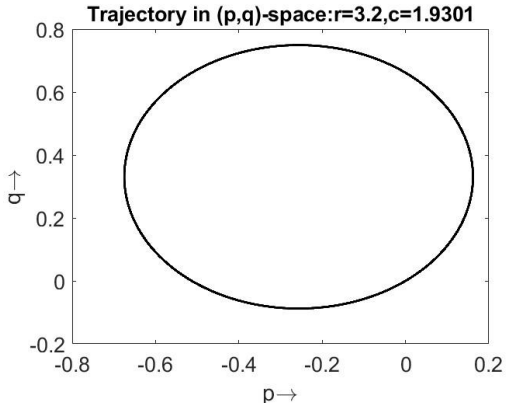

(a)

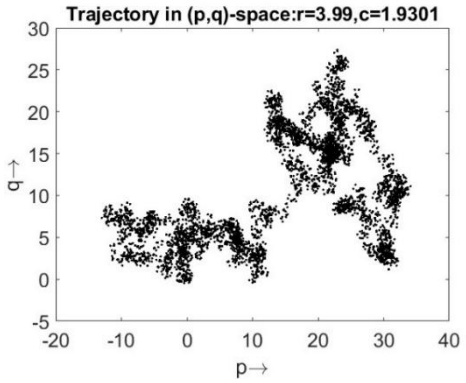

(b)

Figure:1 Plots of p and q for the Logistic map (a) $r = 3.2$, (b) $r = 3.99$

(B). Computation of Mean Square Displacement

Using the translational variables, $p_c(n)$ and $q_c(n)$ as defined ineq.(1),we may define the mean square displacement, $M_c(n)$, for different values of $c \in (0, \pi)$, as [9]:

$$M_c(n) = \lim_{N\to\infty} \frac{1}{N}\sum_{i=1}^{N}[\{p_c(i+n) - p_c(i)\}^2 + \{q(i+n) - q_c(i)\}^2]. \quad (2)$$

The 01CT is based on the growth rate of $M_c(n)$ as a function of n.
Therefore, considering the asymptotic growth rate , K_c , of , $M_c(n)$- the mean square displacement, is as:

$$K_c = \lim_{n\to\infty} \frac{\log M_c(n)}{\log n} \quad (3)$$

where the limit gets assured for $n \leq n_{cut\ off}$, and with $n_{cut\ off} \cong \frac{N}{10}$ yields fairly accurate results [9-11].

In the following section, among the various nonlinear dynamical systems as described by maps and coupled ordinary differential equations, we consider applying the 01CT to only the 1D- Logistic map, 2D-Henon map and sinusoidally excited Duffing systems.

2b. Description of Shanon's Entropy (SE) method

Shanon entropy provides a basis for computing the information dimension of a system

which further characterizes the fractal structure of the system under investigation [4].

Entropy in fact provides a measure of the average amount of information of the state of

the system. Shanon entropy may be computed on binning into cell of an interval of size

unity and thus enabling finding of the probability $p_i = {}^{n_i}/_{N_T}$ that each cell is occupied.

We may therefore write the expression for Shanon's entropy (SE) of the state of a system

as:

$$SE = -\sum_{i=1}^{N_T} p_i \log p_i \ . \quad (4)$$

3. Application of 01CT and SE in some discrete and continuous nonlinear dynamical system

In the following, we describe (a) 1D- Logistic map, (b) 2D Henon's map and (c) a Duffing oscillator excited sinusoidally and the results of applying the 01CT and SE in each cases.

(a) Logistic Model: Verhulst [1] considered the following discrete-time dynamical model,

$$Q_{i+1} = Q + aQ_i(1 - Q) \quad (1)$$

which describes the population size Q_i of say, animals, bacteria etc at discrete times

$$i = 0,1,2,..$$

Assuming that the growth rate of population to be r, a form of the foregoing equation i.e., $\left(\frac{Q_{i+1}-Q_i}{Q_i}\right) = a$, represent a linearly growing population. Verhulst noted that population does not grow linearly, and therefore incorporated a nonlinearity, as in eq.(1), in the formof a quadratic term e.g., $aQ_i^{\,2}$, that limits the linear growth rate. Further normalization with respect to population maximum size results in the following form

$$X_{i+1} = rX_i(1 - X_i), \quad (2)$$

also termed as Logistic equation with $0 \leq X_i \leq 1$ in one dimension Despite its simplicity, logistic mapgenerates very complex behavior as showninFig.1. For instance when $r = 3.2, 3.55, 3.84$ and 3.98 we observe regular, quasi-periodic almost regular and chaotic behavior respectively of the evolution of X, say, population. A peculiar phenomena in nonlinear dynamical system is the'intermittency' which corresponds to sudden transition from almost regular to chaoticbehavior and vice-versa. Fig.2 displays the intermittent behavior in Logistic map. Another important parameter that characterizes transition from order to chaos in a nonlineardynamical system is the existence of a universal called 'Feigenbaum constant'. Forinstancein case of Logistic map, successive change of state (Fig.1) where a period 2^n −cycle appears with increase in r give rise to

the limit

$$\delta = \lim_{n\to\infty} \frac{r_{n+1}-r_n}{r_{n+2}-r_{n+1}} \to 4.6692.$$

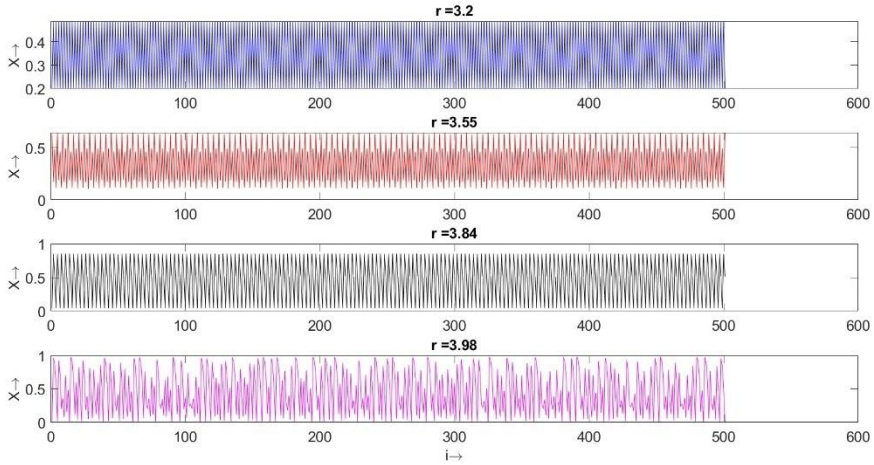

Figure: 1

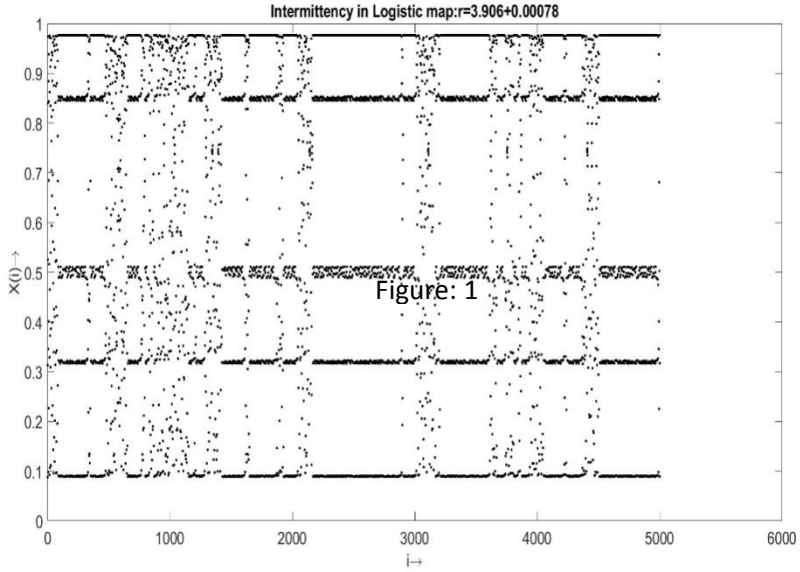

Figure: 1

Figure: 2

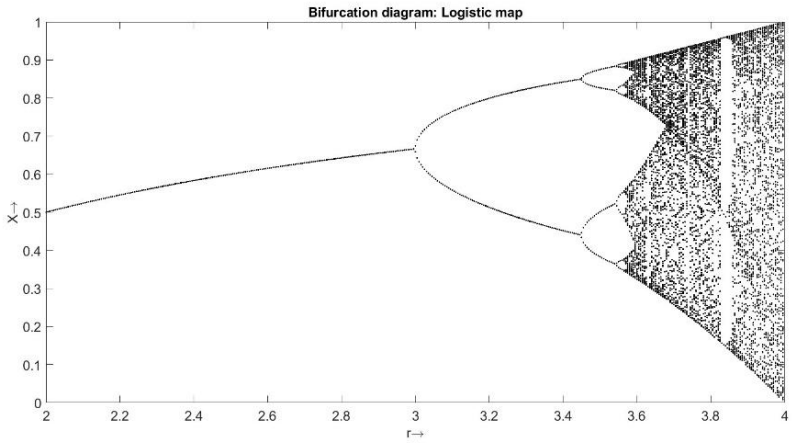

Figure:3

Fig.3 reveals the bifurcation diagram describing the state of the system as the growth rate parameter r is gradually increased from its value of 2.0 to 4.0. This diagram clearly shows the transition from regular dynamics to chaotic dynamics as the parameter r gets increased. However, a conspicuous window around $r \cong 3.84$ is observed where dynamics seems to be regular (Fig.3).

Using the 01CT method, described earlier in section 2a, we computed the growth rate of the mean square displacement, K_c , for randomly chosen 30 values of c in the region $(0, \pi)$. Fig.4,plots the median value, K, of the growth rate [9], further reveals the details of the evolution of complex behavior, as observed in Fig.3, based on 01CT, for $3.5 \leq r \leq 4.0$. It is interesting to observe several sharp windows, in the domain $3.6 < r \leq 4.0$ of the parameter r where there is a possibility regular dynamics in Logistic map.

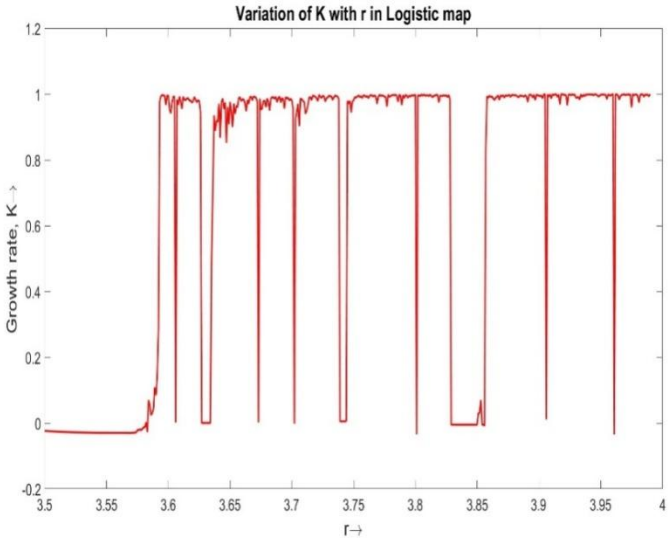

Figure:4

The complexity of a system could be expressed in terms of its 'entropy'. We computed the Shanon entropy, SE, of the Logistic map, shown in Fig.5, which clearly describe regular and chaos observed earlier. It clear demonstrate and characterize the transition from periodic to quasi-periodic- chaotic behavior observed in Logistic map for $2.6 \leq r \leq 4.0$.

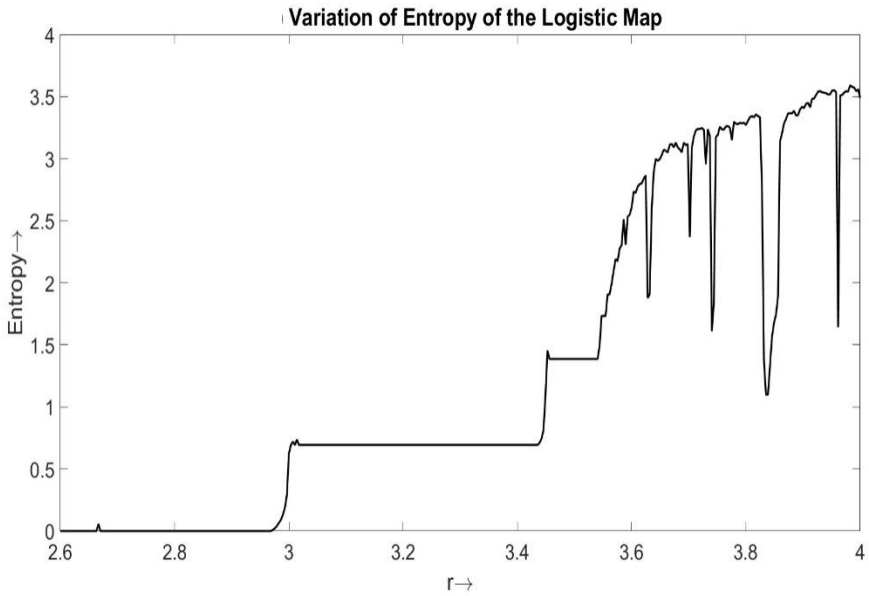

Figure: 5

(b) Henon 2D map : It is among the simplest 2D map that has been extensively used in understanding the stretching and folding dynamics in a chaotic system such as Lorenz system [1,8]. It is described by the following equations,

$$X_{n+1} = 1 - aX_n^{\,2} + Y_n$$
$$Y_{n+1} = bX_n \qquad (3)$$

Fig.6 illustrates the sequence of X values generated when $a = 1.0, 1.1, 1.2$ and 1.4 while $b = 0.3$.The phase space $,(X, Y),$ trajectory for typical values of $a = 1.4$ and $b = 0.3$exhibiting chaotic behavior is displayed in Fig.7. In fact it shows a strange attractor [1]. The bifurcation diagram showing the transition from regular to chaotic behavior with gradual increase in the value of the parameter, a, while keeping the parameter value $b = 0.3$ is shown in Fig.8.

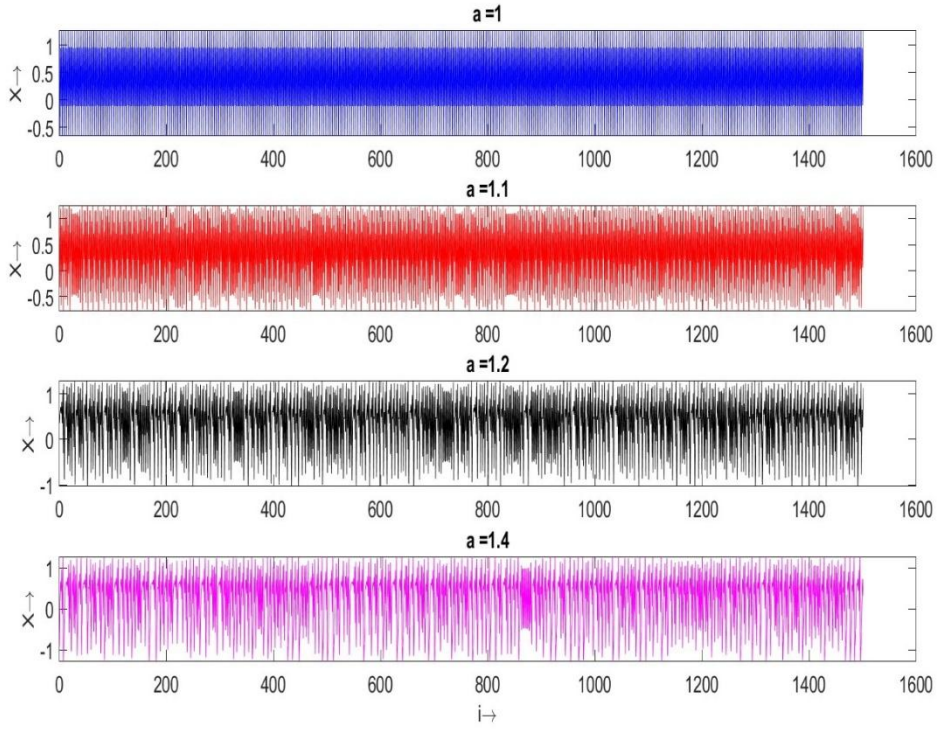

Figure:6

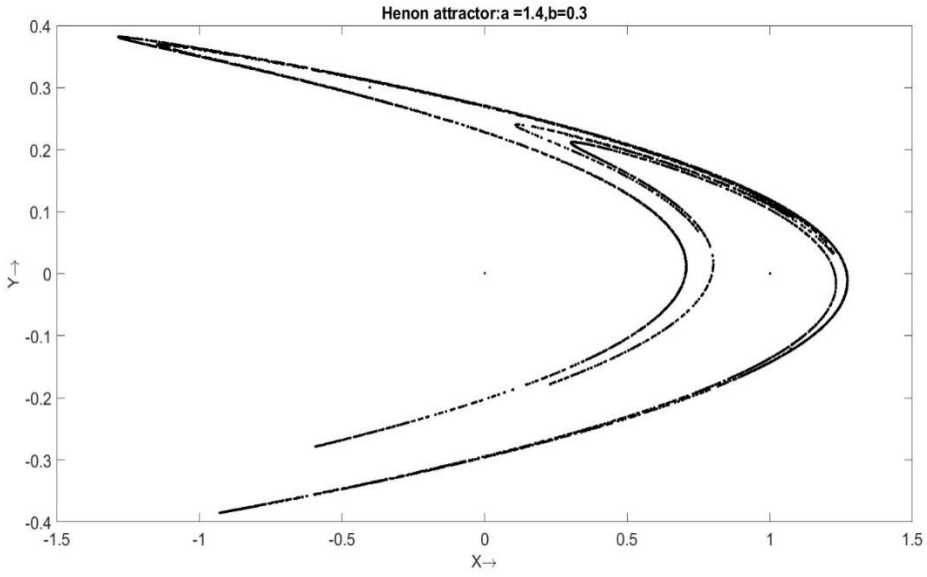

Figure:7

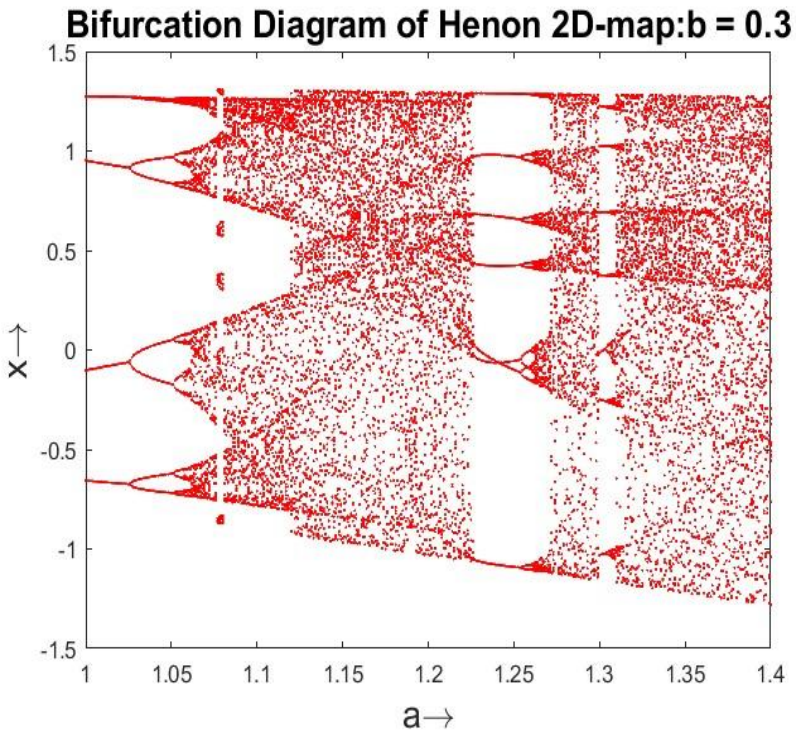

Figure:8

Fig.8 clearly displays the complexity of dynamics in Henon 2D map when $b = 0.3$.

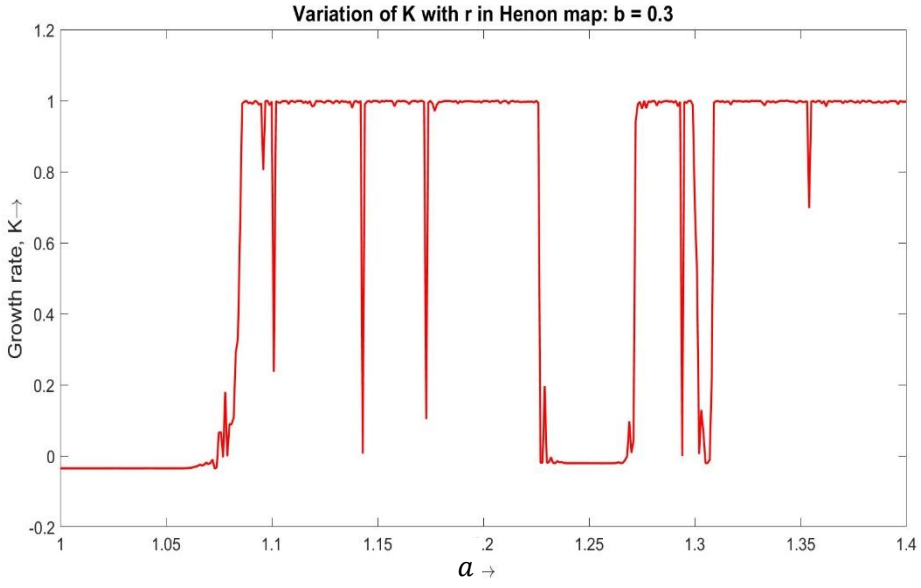

Figure:9

The 01CT when applied to Henon 2D map, effectively characterizes the various transitions observed in the bifurcation diagram of Fig.8. Sharp transition windows are

further visible where the growth rate of mean square displacement, K, drops to ≈ 0 when the control parameter, a, of the system is varied in the range $1.0 \leq a \leq 1.4$.

In addition, the Shanon entropy measure, SE,as shown in Fig.10 further reveals and characterizes various transitions, observed earlier in Fig.8-9.

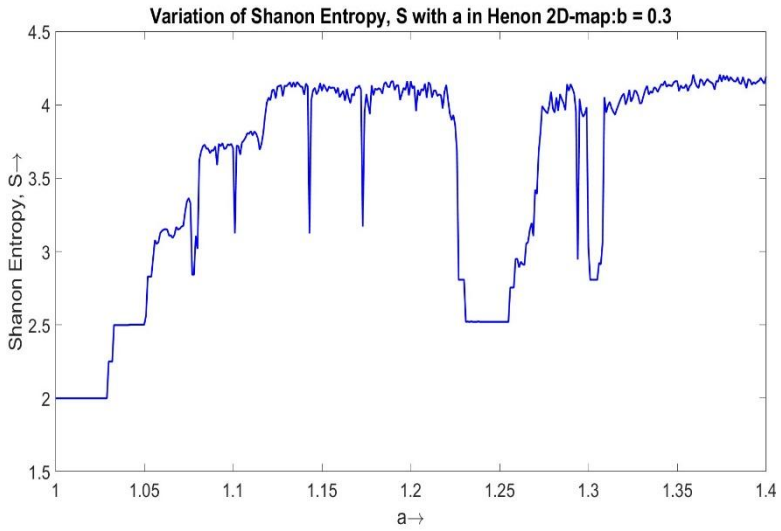

Figure:9

(c) Excited Duffing System

For continuous nonlinear dynamical system, we consider, as an example of a sinusoidally excited Duffing oscillator defined by [12,13,14],

$$\begin{aligned} \frac{dX}{dt} &= Y \\ \frac{dY}{dt} &= X - 2a\,Y - X^3 + F\cos Z \\ \frac{dZ}{dt} &= \omega \end{aligned} \qquad (5)$$

with $a = 0.10$ and $\omega = 1.25$. Fig.10 describe the time series of the displacement variable, X, for different values of the amplitude, F, of the sinusoidal external excitation. Fig.11

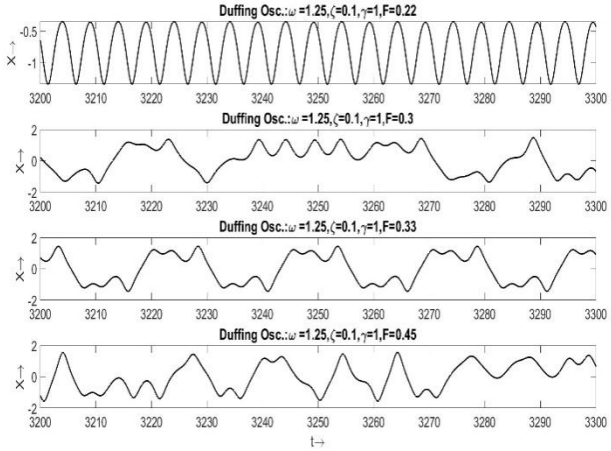

Figure:10

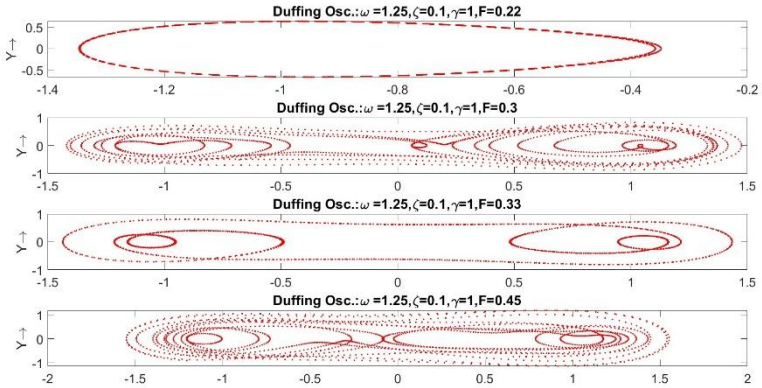

Figure:11

Further displays the phase portrait of the system, eq.(5), for various values of the amplitude, F, of the sinusoidal excitation. Both Fig.10 and Fig.11 describes various transition i.e., periodic to chaotic and chaotic to regular and again regular to chaotic state etc. that takes place in the system as the control parameter, F, increases which further illustrate the complex behavior of the periodically excited Duffing system, eq.(5).

Application of 01CT to the excited Duffing system, clearly characterizes the mean growth rate parameter, K, of the mean-square displacement defined in eq.(2). As per the 01CT, if $K \approx 0$, then the nonlinear dynamical system exhibit regular dynamics while for $K \approx 1.0$, the system is characterized to be chaotic. In case of the present sinusoidally excited Duffing system, from the trend of variation of mean square displacement, K, with F (Fig.12), the dynamics is characterized as regular in the region $0 \leq F \leq 0.25$ and $0.318 \leq F \leq 0.342$ while chaotic dynamics is observed when $0.272 \leq F \leq 0.316$ and $0.342 \leq F \leq 0.486$.

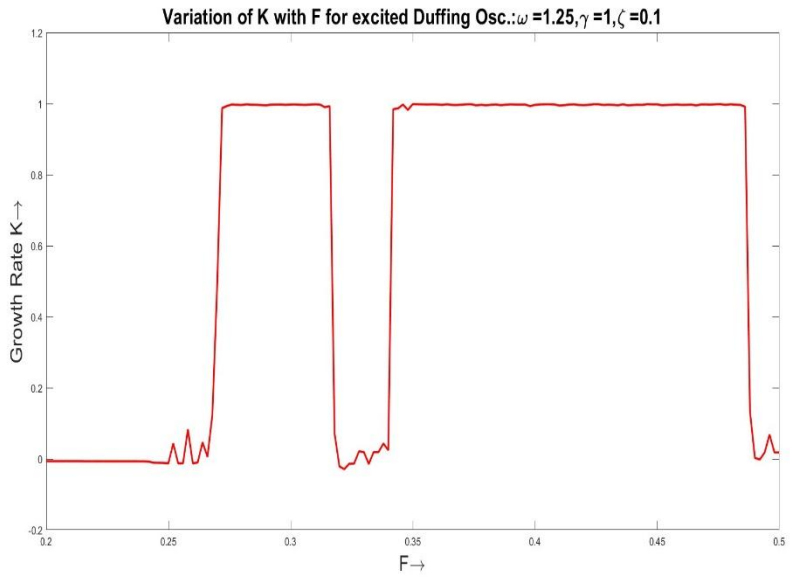

Figure:12

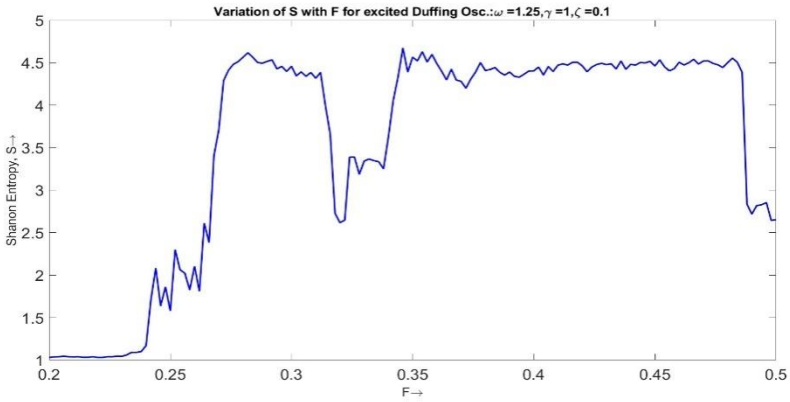

Figure:13

Fig.13 shows the variation of entropy, SE, of the sinusoidally excited Duffing system when the damping coefficient $\gamma = 0.10$ [cf. eq.(5)]. It is clearly able to characterize various transition of the state of the system with increase in, F, as earlier noted in Fig.12 describing the growth rate ,K, of the mean-square displacement in 01CT.

4. Discussion

The problem of characterizing the regular and chaotic nonlinear dynamical system has been addressed using the 01CT and SE technique and as a case study 1D Logistic map, 2D Henon map and excited Duffing system has been chosen as examples of discrete and continuous system. The results obtained in section 3 for different nonlinear dynamical system shows the utility of 01CT and SE to correctly characterizing the complex dynamics observed in the

foregoing system.

References

[1]Buscarino, A., Fortuna, L., Frasca, A., *Nonlinear Circuit Dynamic with MATLAB and Laboratory Experiments*, 2017, CRC Press, Taylor & Francis Group.

[2] Strogatz, S., Nonlinear dynamics and chaos : with applications to physics, biology, chemistry, and engineering, 2001, Westview Press.

[3]Shintani, M., Linton, O., *Is there chaos in the world economy? A non-parameteric test using consistent standard errors*, Tech.Report 0111, Venderbilt University, Department of Economics.

[4] Claycomb, J., Tran, J.Q.P., *Introductory Biophysics- Perspectives on the Living States*,

2011, Jones & Bartlett Publishers.

[5] Abarbanel, H.D., Brown, R., Kennel, M., *Lyapunov exponents in chaotic systems: Their importance and evaluation using observed data*, 1991, Int.J. Mod. Phys., 5, 1347-1375.

[6] Eckmann, J.P., Ruelle, D., *Ergodic Theory of chaos and strange attractors*, 1985, Rev. Mod. Phys. 57, 617-656.

[7] Saha, L.M., Budhraja, M. The largest eigenvalue: An indicator of chaos, 2007, Int.J. Appl.Math. Mech., 3, 61-71.

[8] Gottwald, G.A, Melbourne, I., The 0-1 test for chaos: A review , 2016, Chaos Detection and Predictability, **915**, 221-247, Springer.

[9] Gottwald, G.A., Melbourne, I., On the Implementation of the 0-1 Test for chaos,2009, SIAM J. Appl. Dyn. Sys., **8**, 129-145.

[10] Gottwald, G. A., Melbourne, I., A new test for chaos in deterministic systems, 2004, Proc. Roy. Soc. A, **460**, 603-611.

[11] Gottwald, G.A., Melbourne, I., Testing for chaos in deterministic system with noise, 2005, Physica D, **212**, 100-110.

[12] Fouda, J.S.A.E., Bodo, B., Sabat, S.L., Effa, J.Y., *A Modified 0-1 Test for Chaos Detection in Oversampled Time Series Observations*, 2014, Int.J.Bif.Chaos, **24**, 1450063(13pages).

[13] Das, Sa., Bhardwaj, R., Duhoon, V., *Chaotic dynamics of recharge–discharge El Ni˜no–SouthernOscillation (ENSO) model*, 2022, Eur.Phys.J.Spec.Top., https://doi.org/10.1140/epjs/s11734-022-0742-z.

[14] Das, Saureesh and Bhardwaj, Rashmi,*Recurrence analysis and synchronization of two resistively coupled Duffing-type oscillators*,Nonlinear Dynamics, **104(3)**, 2127-2144.https://doi.org/10.1007/s11071-021-06423-1.

\

 Ganita Sandesh Vol. 34 (June & December, 2020) pp. 38-43 ISSN : 0970-9169

Precise mathematical analysis of bisection method with some relevant software

[1]Dr. Jyoti Singh Raghav, [2*]Dr. Pramod Metha

Department of Mathematics,

[1]Rama University, Kanpur, [2]Mewar University, Rajasthan, India

Email Id:jyotiprashantraghav@gmail.com, pramod_bunty@rediffmail.com

Abstract: In present work wesolve the non linear system of equation using bisection method with the help of three different software viz. MATLAB, SCILABand EXCELsoftware's. The software is quite efficient and practically suited for solving the method. The main aim of study is comparing the rate of performance about the rate of convergence of concerned bisection method on different software's. For this we find the root of the equation $f(x)=\cos x-e^{x}+2x+4$ on a close interval [0, 1]. Using the bisection method, it has been observed that the method used for MATLAB and SCILAB converged in ten iterations while the method used for EXCEL converged in 21 iterations. The current study aimed to conclude that the MATLAB and SCILABsoftware's are more effective in solving the bisection method as compare toEXCEL.

Keywords: Convergence; Roots; Algorithm; Iterations; Bisection Method;

1. Introduction:A system of nonlinear equation is a set of an equation where either one or more than one variable of degree two or moreis a multiplication of variables in one of them. Most realistic and useful systems like weather i.e. $x^{2}+x+1=0$ [1].

The transcendental equation is an equation containing transcendental functions (for example exponential, logarithmic, trigonometric, or inverse trigonometric functions) of unknowns. Root-finding process may be used to get optimum solutions for these equations.i.e. $x=e^{-x}, x=\cos x, 2^{x}=x^{2}$ [2].

The problem of root-finding has remained most appropriate of almost all computational problems. This is because the root-finding problem has often manifested in a wide ranges of practical applications like Physics, Chemistry, Bioscience and Engineering etc.

What gives rise to the root-getting process is the need for determination of every unknown that appears implication in scientific or engineering formulas [3].

There are several relevant situations in physics where such problems need to be solved. Such situations comprise finding the optimum condition of an object, quantized energy level of confined structure[4].

There are several methods to get the non- linear system such as Newton-Raphson, Bisection, False- Position, Secant Method. The rate of convergein all methods are differ than others.Somemathematical methods are quickerto find converging of the root than others. The rate of convergence may be linear or quadratic or else[5]. The study is comparing the rate of performance of MATLAB, SCILAB, and EXCEL software's by using the Bisection Method of root-finding.

The name MATLAB is a high-performance language for numerical computing. It simulates computation, visualization as well as programming insimple to use surroundings where concerned problems and solutions are articulated in precise mathematical notation.

In thescholasticsurroundings it's the standard tool for fundamental and advanced studies in the field of, engineering, mathematics, science and in industry. It isconsidered a high tool of choice for productivity research, developmentalong with analysis[6].

SCILAB is a without chargeapplication along with Open-Source software which includes hundreds mathematical functions. It is used toget the better computing environment in engineering and scientific fields [7].

Microsoft EXCEL is considered a spreadsheet functioning to collected data. It is generally used to generate much type of grids concerned to text, numbers along with required formulas and calculations. It's beneficial for mostly businesses, which examined spend money and income, course of actionin budgets, chart data, along with succinctly present financial consequences.MS EXCELis also having precisely and reasonable programming,used to develop relatively fascinated financial and scientific computing [8].

The Bisection technique is considered as one of the easiest root-solving algorithms, used to get zeros of continuous and nonlinear functions. This approach is very precise and generally gives the optimum solution, ifthe symbols of the function are dissimilar at the chosen initial interval.Unfortunately, it is having only and only one linear convergence, formore accuracy, it doubles with every iteration, which becomes proportionallyslow. Hence, it is frequently used to getinitial calculation for root-solving methods, having a precise rate of convergence. Bisection method may be implementing for non-differentiable and continuous functions.

This method is totally based on repeated frequent bisections of an interval, having the roots[9].

1.1 Algorithm of Bisection technique for Root Solving

Input: (i) $f(x):-$ the required function

(ii) $a_0, b_0 :-$ Two numbers i.e. $f(a_0)\,f(b_0)<0$

Output: - an approximation of the root of $f(x)=0$ in $[p_0, b_0]$. For $\sum_0^\infty k$ do until satisfied:

- Compute $p_k = \dfrac{a_k + b_k}{2}$
- Test if p_k is required root, if so, process must stop.
- If p_k isn't required root, testing for $f(p_k)\,f(a_k)<0$ if so, $b_{k+1}=p_k$ and $a_{k+1}=a_k$ otherwise, set $a_{k+1}=p_k$, $a_{k+1}=a_k$.

1.2 Stopping Criteria

As it is an iterative process, we should work on the stop criteria that will provide the permission to stop this iteration. We have utilized some specific criteria to get better result.

Let ε be the tolerance. i.e., we have obtained the root finding with amathematical error ε. Then accept $x=p_k$ as a required root of $f(x)=0$ if any one of the following mathematical criteria isfulfilled:-

(i) $|f(p_k)|\le\varepsilon$ (The functional variant numerical value is less than or else equal to the tolerance).

(ii) $\dfrac{|p_{k-1}-p_k|}{|p_k|}\le\varepsilon$ (The relative variant numerical value is less than or else equal to the tolerance)

(iii) $\dfrac{b-a}{2^k}\le\varepsilon$ (The extent of the gap after fix k iteration is always less than or else equal to tolerance)

(iv) The numeral of iteration k $\ge$ predetermined number, considered as N.

The number of iteration need in bisection process to get optimum certain accuracy.

1.4 Theorem: Iterations N required in bisection process to get an optimum accuracy of ε is

$$N \ge \frac{\log_{10}(b_0-a_0)-\log_{10}\varepsilon}{\log_{10}2}$$

Proof: Let the interval extent after N iterations are $\dfrac{b_0-a_0}{2^N}\le\varepsilon$

That is $2^{-N}\left(b_0-a_0\right)\le\varepsilon\Rightarrow 2^{-N}\le\frac{\varepsilon}{\left(b_0-a_0\right)}$

$$-N\log_{10}2\le\log_{10}\frac{\varepsilon}{\left(b_0-a_0\right)}\Rightarrow N\log_{10}2\ge-\log_{10}\frac{\varepsilon}{\left(b_0-a_0\right)}$$

$$N\ge\frac{-\log_{10}\frac{\varepsilon}{\left(b_0-a_0\right)}}{\log_{10}2}\Rightarrow N\ge\frac{\log_{10}\left(b_0-a_0\right)-\log_{10}\varepsilon}{\log_{10}2}$$

Hence proved [10]

2. Analysis and Discussions:

The bisection method was applied to a single-variable function: $f\left(x\right)=\cos x-e^{x}+2x+4$ on [0, 1] using the software, MATLAB, SCILAB, and EXCEL, presented in Table 1 to 3.

Table 1: Iteration Output of Bisection by Using MS EXCEL

Iteration	**XL**	**XU**	**XR**	**F(XL)**	**F(XR)**	**F(XU)**
1.	0	1	0.5	4	4.228861	3.82202
2.	0.5	1	0.75	2.228861	4.114689	3.82202
3.	0.75	1	0.875	1.114689	3.992122	3.82202
4.	0.875	1	0.9375	0.492122	3.913216	3.82202
5.	0.9375	1	0.96875	0.163216	3.869181	3.82202
6.	0.96875	1	0.984375	-0.00582	3.845995	3.82202
7.	0.96875	0.984375	0.976563	-0.00582	3.857686	3.845995
8.	0.96875	0.976563	0.972656	-0.00582	3.863458	3.857686
9.	0.96875	0.972656	0.970703	-0.00582	3.866326	3.863458
10	0.96875	0.970703	0.969727	-0.00582	3.867755	3.866326
11.	0.96875	0.969727	0.969238	-0.00582	3.868468	3.867755
12.	0.96875	0.969238	0.968994	-0.00582	3.868825	3.868468
13.	0.96875	0.968994	0.968872	-0.00582	3.869003	3.868825
14.	0.96875	0.968872	0.968811	-0.00582	3.869092	3.869003
15.	0.96875	0.968811	0.968781	-0.00582	3.869137	3.869092
16.	0.96875	0.968781	0.968765	-0.00582	3.869159	3.869137
17.	0.96875	0.968765	0.968758	-0.00582	3.86917	3.869159
18.	0.96875	0.968758	0.968754	-0.00582	3.869176	3.86917

19.	0.96875	0.968754	0.968752	-0.00582	3.869178	3.869176
20.	0.96875	0.968752	0.968751	-0.00582	3.86918	3.869178
21.	0.96875	0.968751	0.96875	-0.00582	3.86918	3.86918

Table 2: Iteration Data of Bisection by Using MATLAB

Iteration	**Low**	**High**	**X_0**
0	0.000000	1.000000	0.500000
1	0.500000	1.000000	0.750000
2	0.750000	1.000000	0.875000
3	0.875000	1.000000	0.937500
4	0.937500	1.000000	0.968750
5	0.968750	1.000000	0.984375
6	0.984375	1.000000	0.992188
7	0.992188	1.000000	0.996094
8	0.996094	1.000000	0.998047
9	0.998047	1.000000	0.999023

Table 3: Iteration Data of Bisection by Using SCILAB

Iteration	Low	High	Z
0	0.000000	1.000000	0.500000
1	0.500000	1.000000	0.750000
2	0.750000	1.000000	0.875000
3	0.875000	1.000000	0.937500
4	0.937500	1.000000	0.968750
5	0.968750	1.000000	0.984375
6	0.984375	1.000000	0.992188
7	0.992188	1.000000	0.996094
8	0.996094	1.000000	0.998047
9	0.998047	1.000000	0.999023

3. Conclusion:

In this study, the bisection method fornon linear equation $f(x) = \cos x - e^x + 2x + 4$ on [0,1] is computed with the help of three softwareMATLAB, SCILAB and MS EXCEL.The efficiency ofeach software is considered as several iterations of it, in solving the bisection method. From the above mentioned tables, analyzed the number of bisection iteration of each software. In comparing the results based on the three software's, it has been observed that the number of iterations produced by MATLAB and SCILAB software is 10 while the number of iterations produced by EXCEL is 21. The discussion presented and results found, it is concluded that MATLAB and SCILAB software is faster and more effective in solving the bisection method than EXCEL software. When we compare the MATLAB and SCILAB, the SCILAB is open resource which is available for everyone and anywhere.

References:

[1] hpps://www.quora.com 8:00 PM, 2, May 2020

[2]Wikipedia, the free encyclopedia. 12:30 AM, 1 May 2020

[3] Datta,B.,lecture notes on numerical solution of root finding problems, (2012), www.math.niu.edu/dattab.

[4] Iwetan,C.N.,Fuwape,I.A.,Olajide,M.S. andAdenodi,R.A.,Comparative study of the Bisection and Newton Methods in solving for zero and extremes of a single-variable function. J of NAMP (2012), vol. 21, 173-176.

[5] Charle, A. and Cooper,W.W., Non-linear power of Adjacent Extreme points methods in linear programming, Econometrica,(2008), vol.25(1), 132-153.

[6] https://cimss.ssec.wisc.edu 5, May, 2020.

[7] www.SCILAB.org 10:00 PM 6 May,2020

[8] https://smallbusiness.chron.com11:00 PM 7 May,2020 ;

[9] Daniel, B.,and Stephan, G., Bisection method in Higher Dimensions and the efficiency number, Periocica polytechnic, (2012), vol. 56/281-86.

[10]L.B Richard, and J.F Douglas, Numerical method Analysis, ninth edition: (2011) brooks/ colecengage leaning.

Vol. 34 (June & December) 2020

RAJASTHAN GANITA PARISHAD

राजस्थान गणित परिषद

The Sequence